

Control Strategies for Photovoltaic Energy Storage Systems

Yun-Sheng Tsai,¹ Te-Sheng Hung,² Cheng-Chien Kuo,¹ and Hung-Cheng Chen^{3*}

¹Department of Electrical Engineering National Taiwan University of Science and Technology
No. 43, Keelung Rd., Sec. 4, Da'an Dist., Taipei City 106335, Taiwan

²Graduate Institute of Energy and Sustainability Technology, National Taiwan University of Science and Technology,
No. 43, Keelung Rd., Sec. 4, Da'an Dist., Taipei City 106335, Taiwan

³Department of Electrical Engineering National Chin-Yi University of Technology
No. 57, Sec. 2, Zhongshan Rd., Taiping Dist., Taichung 411030, Taiwan

(Received October 20, 2023; accepted March 6, 2024)

Keywords: energy storage systems, photovoltaic energy storage systems, second-peak load, duck curve

In recent years, with the impact of global climate change and specific commitments, such as the European Climate Law, to reduce greenhouse gas emissions by 55% from 1990 levels by 2030, renewable energy has become an indispensable application in achieving carbon emission reduction goals. Taiwan has also been actively promoting the development of renewable energy, with a target to reach 20 GW of solar power generation by 2025. With a large amount of renewable energy integrated into the grid, its intermittent and unpredictable nature poses significant challenges to grid stability and power dispatch, particularly evident in the formation of the duck curve during the second-peak load period. Balancing power supply and demand is a critical issue, especially after the sun sets. To address this problem, the Taiwan Power Company has proposed the construction of solar energy storage systems (ESSs), and this study is focused on the development of a solar ESS controller using a programmable logic controller platform along with power sensors. The controller is designed to measure the real-time power generation of solar photovoltaic systems and to develop a control strategy for the ESS. It enables the solar photovoltaic system to charge the ESS during the day and discharge it during the second-peak load period. This approach not only helps mitigate the challenges of second-peak load power dispatch but also enhances the utilization of power lines effectively.

1. Introduction

To meet its 2050 net-zero emissions goal, Taiwan is planning to increase the share of renewable energy to 60 to 70%.⁽¹⁾ Taiwan's renewable energy development is mainly focused on solar photovoltaic and offshore wind power installations. However, renewable energy generation is intermittent and less predictable owing to factors such as day–night cycles and seasonal variations.^(2,3) This means that future electricity generation will rely more on weather-dependent sources, making load and renewable energy generation forecasting even more challenging.

As a significant amount of renewable energy is integrated into the grid, its intermittency will impact the supply–demand balance of the power system and grid operation. Mild impacts may

*Corresponding author: e-mail: hcchen@ncut.edu.tw
<https://doi.org/10.18494/SAM4732>

lead to system frequency instability and regional grid voltage fluctuations, whereas severe impacts can result in transmission line congestion and regional grid voltage instability.^(4,5) As mentioned in Refs. 6 to 9, when the large-scale integration of renewable energy generation occurs, the power system becomes difficult to stabilize and control. It will lead to a significant increase in demand for energy storage systems (ESSs).

It has been pointed out that traditional power systems were originally designed for stable power generation in large power plants.^(10–12) Despite this, their ability to quickly adjust power generation is low, and their regulation capability is limited. However, as a result of the rapid changes in intermittent renewable energy generation, traditional power systems will encounter technical problems, primarily related to power quality.⁽¹³⁾ In the literature,⁽¹⁴⁾ the extensive integration of renewable energy is explained to have profound impacts on the power system. The large-scale integration of solar photovoltaic systems, in particular, is anticipated to result in a deterioration of power quality, which is related to stability and reliability and render the system challenging to maintain in a stable operational state. The integration of renewable energy poses new challenges for the power system, yet simultaneously presents opportunities for the utilization of ESSs to address these challenges and propel the power system towards a more sustainable and stable trajectory.

With the increasing integration and penetration of renewable energy sources, various countries have been promoting large-scale ESSs to mitigate the potential impacts of large-scale renewable energy integration into the grid.^(15,16) In the literature,^(17,18) it has been pointed out that ESSs can effectively alleviate the difficulties in balance caused by renewable energy generation in the power system. Das *et al.*⁽¹⁹⁾ emphasized the contribution of ESSs to enhancing the overall performance of the distribution grid. These systems play a crucial role in addressing peak energy demand, facilitating the integration of renewable and distributed energy sources, assisting in power quality management, and reducing the costs associated with grid expansion. In Ref. 20, ESSs are proposed as a solution to enhance power quality by mitigating load variability, thereby improving both power quality and stability. Lund *et al.*⁽²¹⁾ explored strategies for addressing the high variability of renewable energy, with ESSs being regarded as a pivotal solution. Various methods and technologies have been proposed to enhance the flexibility of ESSs, aimed at balancing the instability of renewable energy. In Ref. 21, multiple energy storage technologies were discussed, including batteries, pumped-storage hydroelectricity, and hydrogen, along with an exploration of their advantages, disadvantages, and application scenarios.

In the literature, various methods for controlling the integration of photovoltaics (PV) with distributed ESSs have been proposed, for instance, a coordinated control approach designed to enhance the voltage quality of residential distribution grids by leveraging both PV and battery ESSs (BESSs).⁽²²⁾ Wang *et al.*⁽²³⁾ proposed the use of distributed ESSs to address voltage fluctuations caused by rooftop PV systems in low-voltage distribution grids. The suggested coordinated control method encompasses both distributed and localized control, ensuring effective voltage regulation under various operating conditions while leveraging the capacity of the ESS. Zeraati *et al.*⁽²⁴⁾ proposed a coordinated control strategy that utilizes BESSs to address voltage rise issues in distribution grids with high photovoltaic resource penetration. The

controller effectively employs energy storage capacity under different conditions, ensuring that the voltage of supply lines remains within permissible ranges.

In accordance with the relevant standards advocated by the Ministry of Economic Affairs to promote the integration of solar photovoltaic power generation systems with energy storage devices, we aim to design a photovoltaic ESS controller. Using solar power generation data and information on the ESS's status, control strategies are formulated to store the electrical energy generated by solar PV in the ESS during daylight hours. Subsequently, during the nighttime second peak after the sun has set, controlled discharge is orchestrated to feed power back into the grid. This approach not only addresses the intermittent power supply issue and challenges associated with the nighttime second peak in solar PV but also enhances the efficiency of the transmission lines.

2. Photovoltaic ESSs

As Taiwan undergoes its energy transition, there has been a change in peak electricity consumption patterns as a result of the integration of renewable energy sources. The Ministry of Economic Affairs aims to promote the combination of solar photovoltaic systems with ESSs.⁽²⁵⁾ This encourages existing solar photovoltaic installations to be equipped with ESSs, which would allow the electrical energy generated by solar photovoltaic systems during the day to be used at night, increasing nighttime power supply capacity and the overall capacity of solar photovoltaic installations.

The primary goal of the photovoltaic ESS is to transfer the electrical energy generated by solar PV during the day to nighttime use. Besides effectively alleviating the pressure on nighttime second-peak power supply, redistributing some of the electrical energy for nighttime use also allows for a larger solar photovoltaic energy capacity to be integrated into the grid during the day. This approach can improve the utilization of the same transmission line, release the saturated capacity of the transmission line to some extent, and optimize the ESS's operation.

The operation curves of the photovoltaic ESS are shown in Fig. 1. The principles governing the operation of the photovoltaic ESS comprise the following five points.

- (1) When the solar photovoltaic generation capacity exceeds the capacity contracted with the Taiwan Power Company, the surplus energy beyond the contracted capacity needs to be stored in the ESS. This excess energy is used to charge the ESS and ensure the safe operation of the system.
- (2) Between 10:00 and 14:00 each day, even if the solar photovoltaic generation capacity does not exceed the contracted capacity, operators are allowed to decide freely whether or not to charge the ESS during this period.
- (3) The schedule for discharging during the nightly second-peak hours is planned quarterly. The Taiwan Power Company (Taipower) announces the two-hour second-peak discharge time for the next quarter at the end of each quarter, where each quarter corresponds to December to February, March to May, June to August, and September to November. Taipower regularly publishes the discharge schedule.
- (4) During the start and end of the nightly second-peak discharge, a ramp rate of 5% per minute is required. The time during the 5% ramping period is not counted within the planned two-hour time frame mentioned earlier.

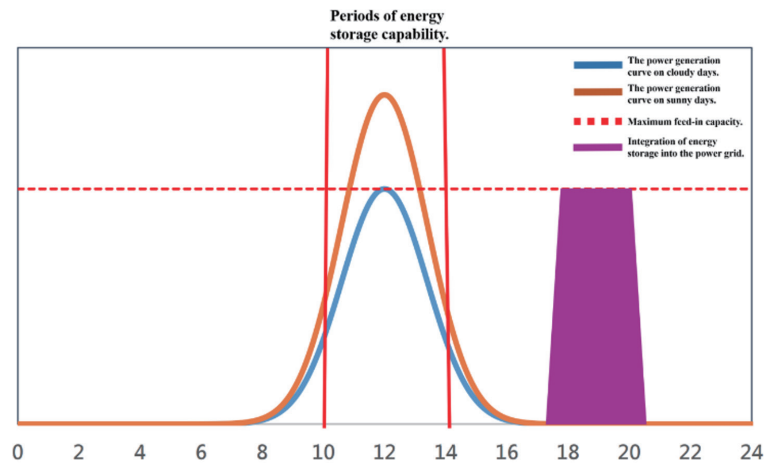


Fig. 1. (Color online) Curve illustrating the operation of photovoltaic ESSs.

- (5) The ESS equipment must comply with Taipower's energy storage interconnection technical guidelines and feed back monitoring information to the ESS controller.

3. Controller of Photovoltaic ESSs

3.1 Introduction to hardware

We use hardware components and equipment developed and produced by FATEK (Yuan Hung Electric Corporation) for the light storage system controller, including a high-performance programmable logic controller (PLC) host, ethernet network module, RS485 communication module, and human machine interface (HMI). Below, we introduce the hardware devices of the light storage system controller.

3.1.1 High-performance PLC host

The high-performance PLC host used as the basis in this research is the FBs-20MCR shown in Fig. 2. The FBs-20MCR high-functionality PLC host possesses the following features:

- (a) The FBs-20MCR high-functionality PLC host features 12 points of 24 V direct current digital input points and eight relay R/T/S output points. Among these, four input points are high-speed 200 kHz points, two input points are medium-speed 20 kHz points, and six input points are medium-speed 5 kHz points.
- (b) There is one RS232 or USB communication port, and it can be expanded to a maximum of five communication ports.
- (c) The FBs-20MCR main unit has a built-in real-time clock (RTC) that can keep accurate time whether the PLC is powered or in a power outage situation. It provides time parameters including week, year, month, day, hour, minute, and second, totaling seven different time values.



Fig. 2. (Color online) FBs-20MCR PLC.

3.1.2 Ethernet network module

The Ethernet network module used is the FBs-CBEH model shown in Fig. 3. This FBs-CBEH network module is a compact and space-saving CPU application expansion module. Through this network module, FBs-CPU can actively or passively communicate with controllers or computers on the Ethernet network. This network module facilitates tasks such as PLC program editing and remote monitoring and diagnostics.

3.1.3 RS485 communication module

The RS485 communication module used in the controller is the FBs-CM55 model. This communication module allows for the expansion of two RS485 communication ports for the FBs-20MCR high-function PLC main unit, providing additional device connectivity.

3.1.4 HMI

The HMI used in the controller is the P2070SK model shown in Fig. 4. This HMI features a seven-inch touchscreen display with a resolution of 800×480 . It is designed with fanless cooling and offers high resistance to noise interference. When paired with the PLC main unit, this HMI allows for convenient control and operation of the controller's settings. It also enables real-time monitoring and display of various power-related parameters on the interface, providing a user-friendly and intuitive interface for operation.

3.2 Light ESS control strategy

In the proposed light ESS control strategy presented in this paper, a PLC is used as the control platform for development. Firstly, real-time power generation from the current solar photovoltaic modules is measured using power sensors. Then, the obtained real-time power generation data is transmitted to the PLC program via MODBUS/RTU communication. The PLC program evaluates the current power generation, current time, and simulated battery state



Fig. 3. (Color online) FBs-CBEH Ethernet network module.



Fig. 4. (Color online) P2070SK HMI.

of charge (SOC) status to determine whether charging or discharging should be initiated at the moment.

As the experiment does not have actual SOC values for the ESS, SOC values are simulated, and the change in simulated SOC is calculated. The decision-making process is based on the limiting conditions set in accordance with the operating principles mentioned earlier. The program will then switch between charging and discharging modes on the basis of the judgment results.

3.3 Control flow chart

The control flow chart of the light ESS is shown in Fig. 5. When the controller program starts executing, it first initializes the SOC value for the ESS. Then, it uses a multifunctional meter to

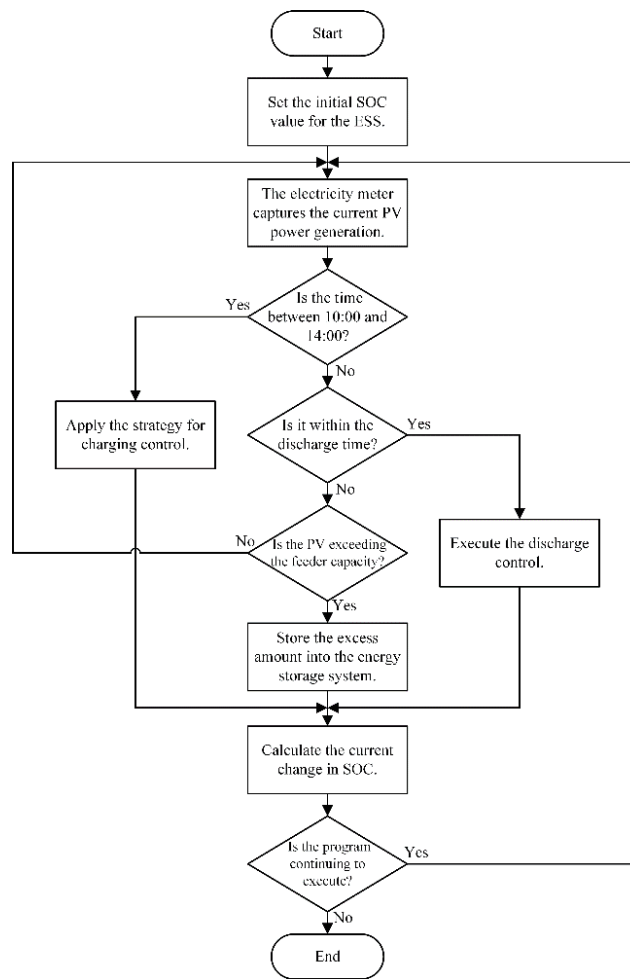


Fig. 5. Photovoltaic ESS control flow chart.

measure the current power generation from the solar photovoltaic modules. The program makes decisions and performs operations on the basis of the current power generation and SOC status, taking into account the predefined limiting conditions.

The controller determines the optimal charging or discharging control for the current time period referring to various judgment results. The controller also calculates the change in SOC for the current state.

3.4 Control limiting conditions

In the control strategy of the light ESS, one of the most critical limiting conditions is related to the SOC protection of the ESS. To protect the ESS within the light ESS, limits are imposed on both the upper and lower bounds of SOC. These limits are set to prevent the controller from overcharging or over discharging the ESS, thus extending its operational lifespan. The upper and lower SOC limits in the light ESS are as follows.

$$\begin{cases} P_{out} \geq 0, & \text{if } SOC_{now} \geq SOC_{max} \\ P_{out} \leq 0, & \text{if } SOC_{now} \leq SOC_{min} \\ P_{out}, & \text{if } SOC_{min} \leq SOC_{now} \leq SOC_{max} \end{cases} \quad (1)$$

Here, SOC_{now} represents the current SOC status, SOC_{max} represents the maximum value of SOC, SOC_{min} represents the minimum value of SOC, and P_{out} represents output power. When SOC_{now} is greater than or equal to the set upper limit SOC_{max} , P_{out} can only be discharged. This means that when SOC_{now} reaches the upper limit, no further charging of the ESS is allowed, and the discharge operation can only be performed in the discharge period. Conversely, when SOC_{now} is less than or equal to the set lower limit SOC_{min} , the ESS cannot be discharged. This ensures that SOC_{now} remains within the range of SOC_{max} and SOC_{min} , thereby protecting the ESS.

3.5 Charging control strategies

To fulfill the charging requirements of the photovoltaic ESS, three sets of charging control strategies have been designed. The activation of these strategies will be determined by assessing the current time and the state of the ESS's SOC. If the current time falls within the 10:00–14:00 time period, and regardless of whether the current electricity generation exceeds the contracted capacity, operators are allowed to freely control the charging process. During this time, the controller will use the designed charging control strategies to regulate the power conversion system (PCS) for charging the ESS. The main purpose of this is to raise the SOC of the ESS to the target value, preparing it for the nighttime second-peak discharge. The flow charts of these three charging control strategies are depicted in Figs. 6–8.

During the open and free charging period, it is necessary to raise the ESS's SOC to the target value to prepare for the two-hour peak discharge period. This period allows for the flexible control of both charging and discharging operations. Therefore, we designed three different charging control strategies.

The main distinction among these strategies lies in the calculation of the charging control quantity, where the α coefficient is used for more refined calculations and judgments. In the case of charging control strategies 2 and 3, different initial values for the α coefficient are used to perform calculations and control. For a comparison of the results and discussions of the different strategies, refer to Sect. 4.

3.6 Peak load discharging control

The discharge control during the nighttime second peak will be determined on the basis of whether or not the current time falls within the nighttime second-peak discharge time announced by Taipower and the battery SOC status. If it is within the nighttime second-peak discharge period, the controller will initiate a two-hour discharge operation for the PCS.

As per the operating principles mentioned in the integration of solar energy storage, peak discharge must have a ramp rate of 5% per minute; this is not counted within the planned two-hour discharge period. Therefore, during this time, the controller will calculate and execute the

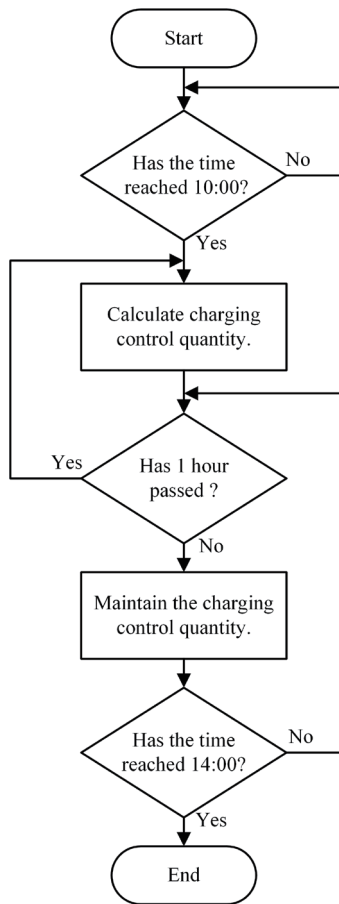


Fig. 6. Charging control strategy 1 for photovoltaic ESSs.

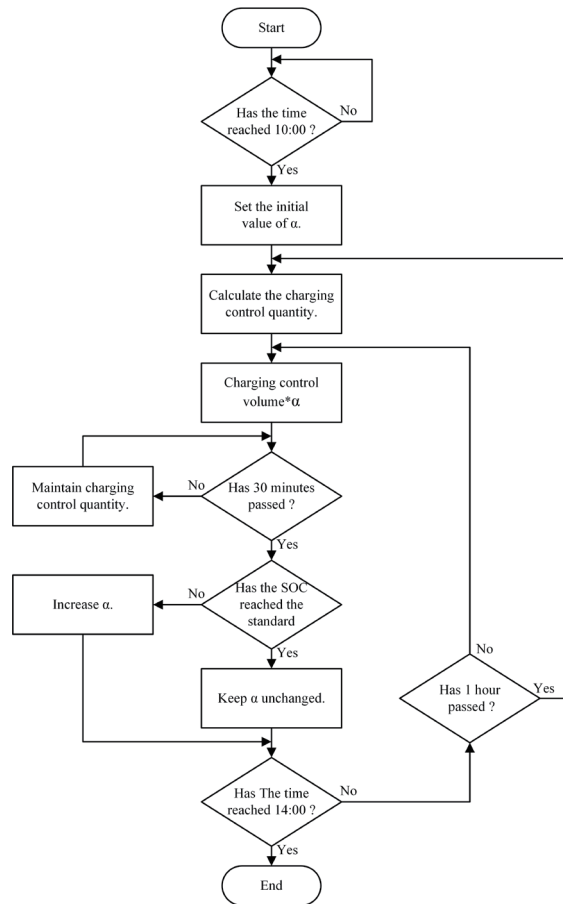


Fig. 7. Charging control strategy 2 for photovoltaic ESSs.

5% per minute ramp-up/ramp-down function for starting and ending the discharge. After ramp-up, continuous discharge will be carried out for two hours.

If the SOC of the ESS falls below the specified minimum value during the discharge process, the discharge operation will be immediately halted to protect the battery and extend the lifespan of the ESS. The peak discharge control flow chart is illustrated in Fig. 9.

3.7 Battery SOC

In the controller designed for the light ESS in this study, it was not possible to measure the actual SOC of the ESS. Therefore, a simulated SOC value was used for testing and experiments. The coulomb counting method was employed to calculate the battery’s SOC.

The coulomb counting method is based on the principle of charge conservation, which states that the total charge in a closed system remains constant. Therefore, when a battery is charged or discharged, its SOC changes in accordance with the variation in the amount of charge entering or leaving the battery. This method is employed to calculate the SOC using the battery’s charging and discharging currents.

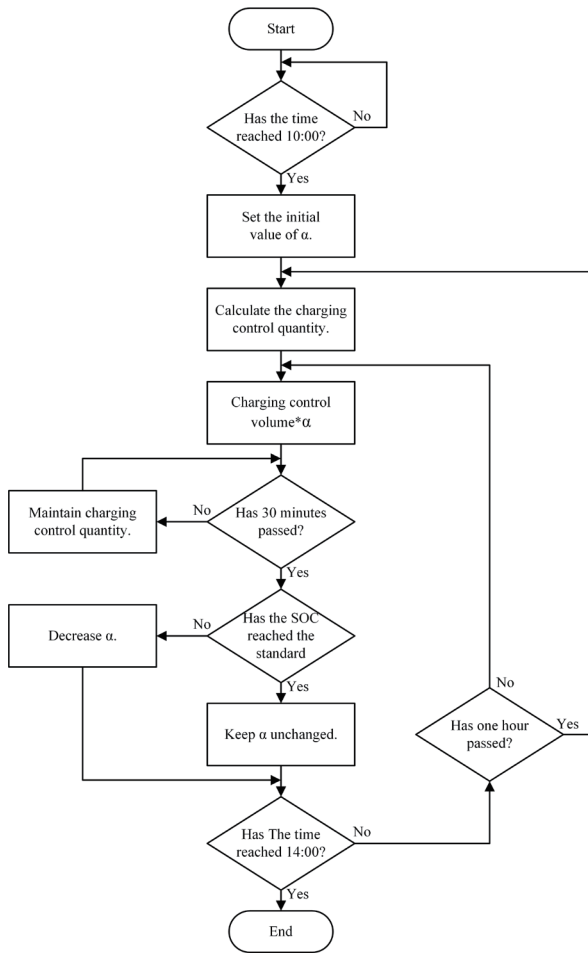


Fig. 8. Charging control strategy 3 for photovoltaic ESSs.

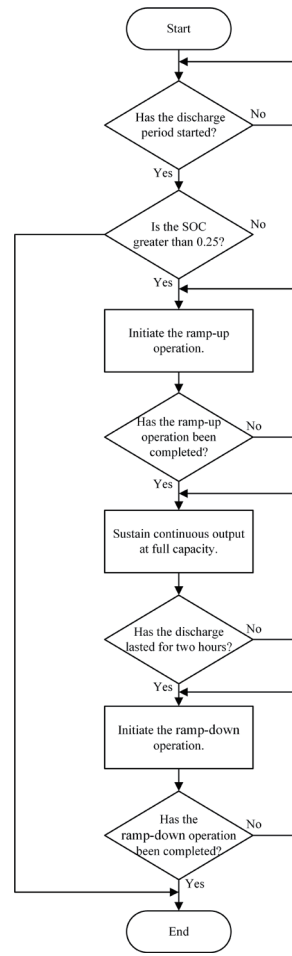


Fig. 9. Peak discharge control flow chart of photovoltaic energy storage.

SOC is calculated by the coulomb counting method as

$$SOC_{now} = SOC_{initial} + \sum \left(\frac{\Delta Q}{Q_{total}} \right) \times 100\%. \tag{2}$$

SOC_{now} represents the current SOC status, while $SOC_{initial}$ signifies the initial SOC value. In our control strategy, simulated values are utilized for $SOC_{initial}$ because of the unavailability of actual battery SOC measurements. Additionally, ΔQ stands for the charge and discharge amounts within each time interval, and Q_{total} denotes the battery's rated capacity, representing the maximum amount of electricity it can store.

4. Test Results and Discussion

The light storage system controller in this study was designed and developed in accordance with the operating guidelines announced by the Ministry of Economic Affairs. Three different charging control strategies for solar photovoltaic systems combined with ESSs were also proposed. In this section, experiments conducted separately for scenarios with and without charging control strategies as well as for the other three charging control strategies are described, and the data obtained from these experiments are analyzed and discussed.

In the experimental testing in this study, power sensors were used to measure solar photovoltaic generation data, and historical data for an entire day was collected. Because of the limited capacity of the experimental equipment's solar photovoltaic generation module, the historical PV generation data was scaled proportionally to better simulate real-world conditions before conducting the experiments. In this testing, it was assumed that the contract capacity was 5 MW, the solar photovoltaic generation capacity was 8.33 MW, and the ESS capacity was 18 MW.

4.1 Comparison of control strategies

Practical control tests were conducted using multiple sets of identical historical data. These tests encompassed scenarios both with and without charging control strategies, and the performances of three distinct charging control strategies were assessed: charging control strategy 1, charging control strategy 2, and charging control strategy 3. For the experimental tests, the initial SOC of the ESS was set at 25%, and the controller began its control actions at 05:00 in the morning, with the peak discharge starting at 17:00 in the afternoon. The charging control and SOC data obtained from the practical control tests were used for discussion and comparison of the scenarios with and without charging control strategies and the three charging control strategies. The following are the test data results and the discussion and comparison of each strategy:

Among the test results for scenarios with and without the inclusion of different charging control strategies, SOC variations are examined to determine whether the charging meets the target. The SOC results for each set of test data are shown in Figs. 10–13 and Table 1. The results in Figs. 10–13 indicate that without any charging control strategy, it is impossible to raise the SOC of the ESS to the target of 90%. With charging control strategy 1, there is an improvement in that SOC is raised to around 80%, but this value still falls short of the 90% target. Charging control strategy 2 successfully raises SOC to the target value. Charging control strategy 3 also successfully raises SOC to the 90% target, and compared with strategy 2, it achieves this target earlier in the test data results. In Fig. 13, the test results show that, even with charging control strategies, it was not possible to reach the target SOC. The reason for this is that the overall generation capacity of historical data D was insufficient, preventing the ESS from attaining the target SOC. The data reveals that when the overall daily generation conditions are unfavorable, the controller can only raise SOC so far, storing as much energy as possible to cope with the second-peak discharge operation.

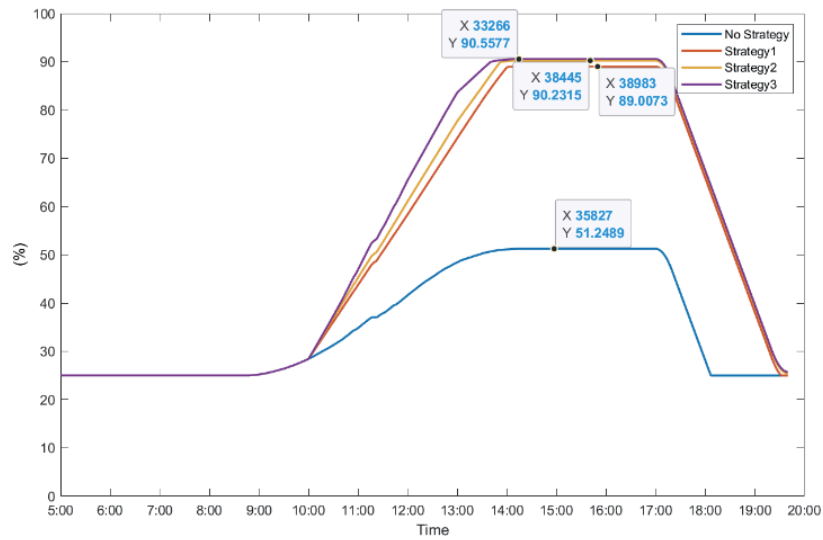


Fig. 10. (Color online) Historical data A. SOC curves of results of each strategy test.

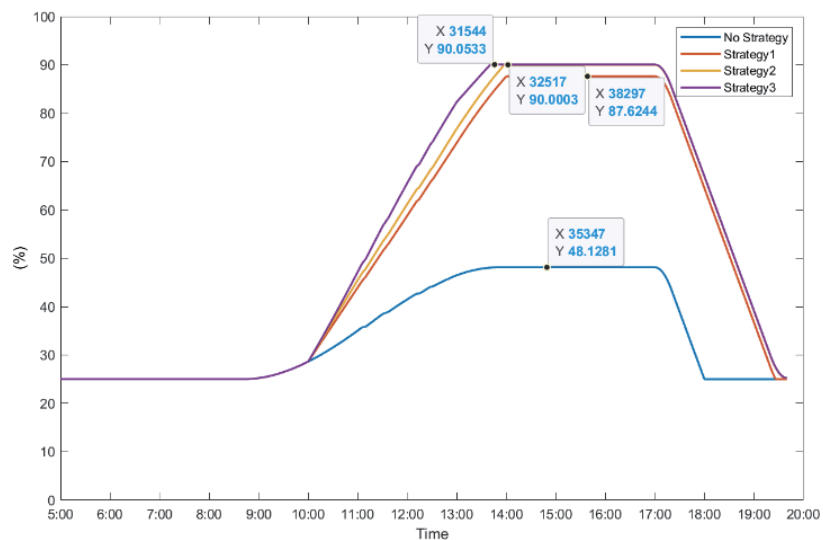


Fig. 11. (Color online) Historical data B. SOC curves of results of each strategy test.

From the results in Figs. 10–13 and Table 1, it is evident that when the controller incorporates charging control strategy 1, there is an improvement in the controller's charging control capability compared with the case of no strategy. However, strategy 1 may still fall short of achieving the target SOC. When the controller adopts charging control strategy 2 or 3, there is a better charging control performance than in the case of strategy 1. Strategies 2 and 3 can effectively charge the ESS to the target SOC and successfully complete the two-hour discharge operation during the nighttime peak period. Therefore, in the control of the photovoltaic ESS, charging control strategy 2 and charging control strategy 3 proposed in this paper are more effective in charging control, aiding the photovoltaic ESS controller to achieve more efficient charging control.

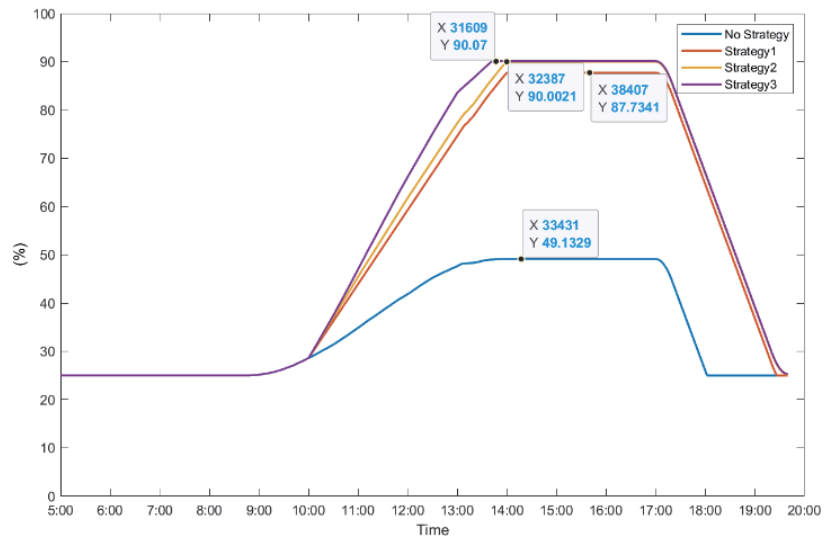


Fig. 12. (Color online) Historical data C. SOC curves of results of each strategy test.

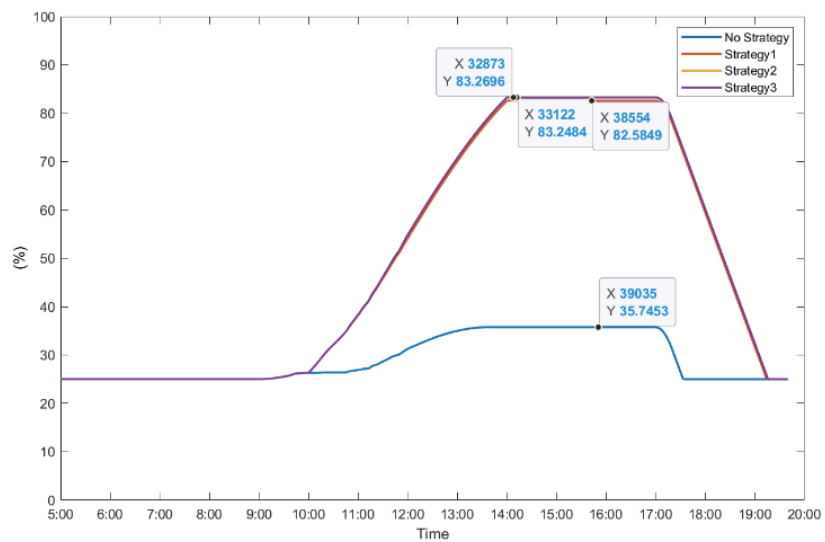


Fig. 13. (Color online) Historical data D. SOC curves of results of each strategy test.

Table 1
Results for each charging control strategy.

Strategy	SOC (%) after completion of charging control			
	Data A	Data B	Data C	Data D
No control strategy	51.24	48.12	49.13	35.74
Control strategy 1	89.00	87.62	87.73	82.58
Control strategy 2	90.23	90.00	90.00	83.24
Control strategy 3	90.55	90.05	90.07	83.26

5. Conclusions

To address the challenges posed by the intermittent nature of renewable energy sources when integrated into the power grid on a large scale in the future, we developed a photovoltaic ESS controller designed for the integration of solar photovoltaic systems with energy storage. This controller was aimed at establishing a more robust distributed energy resource system that can enhance grid resilience. Its goal was to reduce the likelihood of large-scale blackout incidents caused by over-concentration in the power grid.

In the photovoltaic ESS controller, actual solar photovoltaic module generation data were measured using power sensors. The controller's performance was evaluated in various scenarios, including situations with no control strategy and situations with the three charging control strategies proposed in this paper. The changes in ESS SOC and the overall charging and discharging results were compared and analyzed.

The comparison results clearly indicated that, compared with the scenarios with no control strategy and control strategy 1, the inclusion of control strategies 2 and 3 resulted in superior charging control by the controller. The reason behind this improvement was the inclusion of an amplification factor in the charging control calculations. This allowed the controller to maximize SOC during the open charging period to mitigate the potential decrease in solar photovoltaic generation after noon, effectively reducing the chance of SOC not meeting the target.

At this stage, as photovoltaic ESSs are still in the development phase, the controller developed in this study is expected to efficiently store solar energy during the day and inject it into the grid during the evening's second-peak demand. This will contribute to address second-peak power supply challenges, which will help stabilize and strengthen grid resilience. In the future, as solar photovoltaic installations increasingly incorporate ESSs, this controller will play a crucial role in improving grid performance.

Acknowledgments

This research was partially supported by the Ministry of Science and Technology of Taiwan, under Grant MOST 111-2221-E-167-005-MY2.

References

1. Taiwan's 2050 Net Zero Emission Pathway and Strategy Overview: https://www.ndc.gov.tw/Content_List.aspx?n=DEE68AAD8B38BD76 (accessed November 2022).
2. G. Ren, J. Liu, J. Wen, Y. Guo, and D. Yu: Appl. Energy **204** (2017) 47. <https://doi.org/10.1016/j.apenergy.2017.06.098>
3. P. S. Georgilakis: Renew. Sustain. Energy Rev. **12** (2008) 852. <https://doi.org/10.1016/j.rser.2006.10.007>
4. Challenges and Opportunities of Grid Integration for Renewable Energy in Power Dispatch: <https://myppt.cc/FM2N6Q> (accessed November 2022).
5. L. Wang, M. Yuan, F. Zhang, X. Wang, L. Dai, and F. Zhao: IEEE Access **7** (2019) 59653. <https://www.doi.org/10.1109/ACCESS.2019.2912804>
6. R. A. Walling, L. A. Freeman, and W. P. Lasher: Proc. IEEE PES Power Systems Conf. and Exposition (IEEE, 2009) 1–7.
7. G. Strbac, A. Shakoor, M. Black, D. Pudjianto, and T. Bopp: Electr. Power Syst. Res. **77** (2007) 1214. <https://doi.org/10.1016/j.epsr.2006.08.014>

- 8 Y. V. Makarov, C. Loutan, J. Ma and P. de Mello: IEEE Trans. Power Syst. **24** (2009) 1039. <https://doi.org/10.1109/TPWRS.2009.2016364>
- 9 D. A. Halamay, T. K. A. Brekken, A. Simmons, and S. McArthur: Proc. IEEE General Meeting Power and Energy Society (IEEE, 2010) 1–7.
- 10 J. Kabouris, and F. D. Kanellos: IEEE Trans. Sustainable Energy **1** (2010) 107. <https://doi.org/10.1109/TSTE.2010.2050348>
- 11 R. Tonkoski, D. Turcotte, and T. H. M. EL-Fouly: IEEE Trans. Sustainable Energy **3** (2012) 518. <https://doi.org/10.1109/TSTE.2012.2191425>
- 12 E. J. Coster, J. M. A. Myrzik, B. Kruimer, and W. L. Kling: Proc. IEEE **99** (2011) 28. <https://doi.org/10.1109/JPROC.2010.2052776>
- 13 A. Kyritsis, D. Voglitsis, N. Papanikolaou, S. Tselepis, C. Christodoulou, I. Gonos, and S. A. Kalogirou: Renewable Energy **109** (2017) 487. <https://doi.org/10.1016/j.renene.2017.03.066>
- 14 S. Vazquez, S. M. Lukic, E. Galvan, L. G. Franquelo, and J. M. Carrasco: IEEE Trans. Ind. Electron. **57** (2010) 3881. <https://doi.org/10.1109/TIE.2010.2076414>
- 15 P. Zou, Q. Chen, Q. Xia, G. He, and C. Kang: IEEE Trans. Sustainable Energy **7** (2016) 808. <https://doi.org/10.1109/TSTE.2015.2497283>
- 16 T. Weitzel and C. H. Glock: Eur. J. Oper. Res. **264** (2018) 582. <https://doi.org/10.1016/j.ejor.2017.06.052>
- 17 J. P. Barton and D. G. Infield: IEEE Trans. Energy Convers. **19** (2004) 441. <https://doi.org/10.1109/TEC.2003.822305>
- 18 S. Tewari and N. Mohan: IEEE Trans. Power Syst. **28** (2013) 532. <https://doi.org/10.1109/TPWRS.2012.2205278>
- 19 C. K. Das, O. Bass, G. Kothapalli, T. S. Mahmoud, and D. Habibi: Renewable Sustainable Energy Rev. **91** (2018) 1205. <https://doi.org/10.1016/j.rser.2018.03.068>
- 20 S. L. Koh and Y. S. Lim: Energy **101** (2016) 519. <https://doi.org/10.1016/j.energy.2016.02.047>
- 21 P. D. Lund, J. Lindgren, J. Mikkola, and J. Salpakari: Renewable Sustainable Energy Rev. **45** (2015) 785. <https://doi.org/10.1016/j.rser.2015.01.057>
- 22 M. N. Kabir, Y. Mishra, G. Ledwich, Z. Y. Dong, and K. P. Wong: IEEE Trans. Ind. Inf. **10** (2014) 967. <https://doi.org/10.1109/TII.2014.2299336>
- 23 Y. Wang, K. T. Tan, X. Y. Peng, and P. L. So: IEEE Trans. Power Delivery **31** (2016) 1132. <https://doi.org/10.1109/TPWRD.2015.2462723>
- 24 M. Zeraati, M. E. H. Golshan, and J. M. Guerrero: IEEE Trans. Smart Grid **9** (2018) 3582. <https://doi.org/10.1109/TSG.2016.2636217>
- 25 X. Li, L. Wang, N. Yan, and R. Ma: IEEE Trans. Appl. Supercond. **31** (2021) 1. <https://doi.org/10.1109/TASC.2021.3117750>